



# Research on the direct amination of benzene to aniline by NiAlPO<sub>4</sub>-5 catalyst

Wei Wang | Yan Yang | Long Zhang

Jilin Provincial Engineering Laboratory for the Complex Utilization of Petro-resources and Biomass, School of Chemical Engineering, Changchun University of Technology, Changchun 130012, People's Republic of China

## Correspondence

Long Zhang, Jilin Provincial Engineering Laboratory for the Complex Utilization of Petro-resources and Biomass, School of Chemical Engineering, Changchun University of Technology, Changchun 130012, People's Republic of China. Email: zhanglongzhl@163.com

## Funding information

Changchun University of Technology

A series of NiAlPO<sub>4</sub>-5 molecular sieves have been hydrothermally synthesized and shown high and stable activity in the direct amination of benzene to aniline with hydroxylamine hydrochloride as aminating agent. The as-synthesized and calcined samples were investigated with XRD, SEM, TG, BET, NH<sub>3</sub>-TPD and FT-IR to explore the crystalline, coordination and location of the incorporated transition metal ions. The results indicated that nickel ions were incorporated into the framework of AlPO<sub>4</sub>-5 and the as-synthesized catalysts were highly crystalline, and possessed good thermal stability. Among them, Ni(0.3) AlPO<sub>4</sub>-5 showed the highest catalytic activity for the direct amination of benzene with the highest aniline yield of 73.2% and 100.0% selectivity to aniline. After the catalyst was reused for 5 times, the activity remained little change.

## KEYWORDS

aluminophosphate molecular sieves, aniline, benzene, catalytic amination, hydrothermally synthesis

## 1 | INTRODUCTION

Aniline as an important organic chemical raw material and a fine chemical intermediate<sup>[1]</sup> is widely used in the fields of pesticide, dye, pharmaceutical, explosive, spice, resin, rubber additive, special conductive polymer raw materials and the others, especially as the raw material of MDI production. At present, the industrial production of aniline is mainly in three ways, that is, catalytic hydrogenation of nitrobenzene, phenol amination and nitrobenzene iron reduction method, its production capacity is about 85.0%, 10.0% and 5.0% of the total production capacity of aniline, respectively. However, these methods characterized of higher cost, harsh operating conditions and environmental pollution,<sup>[2]</sup> these do not accord with the concept of green chemistry and sustainable development.<sup>[3-5]</sup> Through the activation of C-H bond in benzene, amino groups will be directly introduced into the benzene ring to form aniline.<sup>[6]</sup> By doing it, the multi-step reactions go into a one-step reaction, the entire reaction process can significantly improve the atom utilization, with hydrogen and/or water as by-products.<sup>[7]</sup>

But C-H bond activation is an important and difficult problem to overcome.<sup>[8-11]</sup> Therefore, exploring efficient catalyst system for the direct amination of benzene has attracted more and more attentions in chemical industry recently.<sup>[12-14]</sup> Mantegazza<sup>[15]</sup> has reported the direct synthesis of hydroxylamine with high yield by the oxidation of ammonia with hydrogen peroxide in the presence of Ti-silicate at low temperature and atmospheric pressure. It provided a potential benign supply of hydroxylamine for the amination of benzene. Kuznetsova<sup>[16]</sup> investigated the amination of benzene and toluene with hydroxylamine sulfate in the presence of transition metal redox catalysts in a closed system. The reaction was carried out in acetic acid-water or sulfuric acid-acetic acid-water media, and a maximum aniline yield of about 27% was obtained. Zhu<sup>[2,17]</sup> studied on direct synthesis of aniline with hydroxylamine as aminating agent, inorganic vanadium salts (NaVO<sub>3</sub> or VOSO<sub>4</sub>) and several typical vanadium complexes as catalysts, respectively, with the maximum aniline yield up to 64% and the highest selectivity up to 95.8%; Parida<sup>[18]</sup> studied on the direct amination of benzene to aniline by optimizing the reaction

conditions with hydroxylamine as aminating agent, Mn-MCM-41 as catalyst, the conversion and selectivity to aniline are respectively up to 68.5% and 100%.

Aluminophosphates ( $\text{AlPO}_5$  or  $\text{AlPO}_4\text{-}n$ ) molecular sieves, as one of microporous zeolite family<sup>[19,20]</sup> have attracted wide attention since their first synthesis by Wilson et al. in 1982,<sup>[21]</sup> which is used to describe the 3D oxide frameworks with a 1:1 aluminium-to-phosphorus ratio ( $n$  refers to the specific crystallographic structure). In this sense, the modification of  $\text{AlPO}_5$  framework with transition metal (Fe, Co, Ni, Cu and so on) can lead to the elaboration of novel materials with enhanced acidic and/or redox properties.<sup>[22–27]</sup>  $\text{AlPO}_4\text{-}5$  is a typical aluminophosphate molecular sieve with 3D structure with hexagonal symmetry.<sup>[21,22,28,29]</sup> Yoshihiro Sugi and Ajayan Vinu et al.<sup>[30]</sup> reported the isopropylation of biphenyl to 4,4'-DIPB with Co(5)APO-5 and Ni(5)APO-5 as catalysts, giving the high selectivity to 4,4'-DIPB of 65–75%. Till now there is no report on the direct amination of benzene to aniline with modified  $\text{AlPO}_4\text{-}5$  molecular sieves as the catalyst.

In this paper, Ni doped  $\text{AlPO}_4\text{-}5$  catalyst is explored for one-step amination of benzene to aniline with hydroxylamine hydrochloride as aminating agent in acetic acid aqueous solution, with better results achieved.

## 2 | EXPERIMENTAL

### 2.1 | Materials

Aluminum isopropoxide, phosphoric acid (wt. 85% in aqueous solution), triethylamine, nickel nitrate hexahydrate, benzene, and hydroxylamine hydrochloride, acetic acid, sodium hydroxide, ether and aniline, phenol, nitrobenzene,  $\text{NH}_2\text{OH}\cdot\text{HCl}$  and benzene were all of analytical grade and used without further purification.

### 2.2 | Catalyst preparation

The catalyst was prepared by static hydrothermal method according to literature<sup>[31–35]</sup> after modifications, isopropanol aluminum, phosphoric acid and nickel nitrate hexahydrate as a source of Al, P and metal source, triethylamine as the template. The gel started from the mixture of 1.0 TEA: (0–0.4) NiO: 0.95  $\text{Al}_2\text{O}_3$ : 1  $\text{P}_2\text{O}_5$ : 40  $\text{H}_2\text{O}$ .

The preparation procedure is as follows: metal salts were added to a solution of ortho-phosphoric acid in distilled water at 20 °C. Then, after the transition metal salts were completely dissolved, the above solution was slowly added into the solution of aluminum isopropanol which was per dissolved in water under continuous stirring for

1 hr. Finally, triethylamine as template was dropwise introduced to the above mixture. This mixture was further stirred for 2.5 hr. The resultant gel was sealed in Teflon-lined stainless steel autoclaves in a convection oven and crystallized under autogenous pressure at 200 °C for 16 hr. The as-synthesized solids were filtered, washed with deionized water to neutral, and further dried in air at 90 °C. Then the solid was calcined in an oven in air at 550 °C (at the rate of 3 °C/min rise) for 16 hr, the calcined samples were stored for further use.

### 2.3 | Characterization of the catalyst sample

The crystalline phase of the as-synthesized solids was identified with a D/Max 2000/PC X-ray diffractometer with Cu Ka radiation, pipe voltage is 60 kV, electric current is 330 mA. The spectra were collected stepwise in the range of  $5^\circ \leq 2\theta \leq 50^\circ$ , scan rate  $4^\circ\cdot\text{min}^{-1}$ . Thermal gravimetric analysis was carried out in a STA 6000, under the nitrogen atmosphere at  $20\text{ mL}\cdot\text{min}^{-1}$ , observing the weight loss while the temperature heated from room temperature to 800 °C at the rate of  $10^\circ\text{C}\cdot\text{min}^{-1}$ . The nitrogen adsorption/desorption measurement was performed on a Micromeritics ASAP 2020 M surface area and porosity analyzer. SEM was conducted in a JSM-5500LV high resolution scanning electron microscope, accelerating voltage 0 to 30 kV, resolution of 3.0 nm, 300000–350000 times magnification. The acidities of the catalysts were measured by temperature-programmed desorption using ammonia as the probe molecule ( $\text{NH}_3$ -TPD, Micromeritics AutoChem II 2920). 0.1 g of the sample was placed in a quartz sample tube and heated to 500 °C for 1 hr in helium atmosphere, then cooling to 110 °C. When the temperature was decreased to 110 °C,  $\text{NH}_3$  was introduced to attain adsorption saturation. Then, the sample was purged by helium for 1 hr to remove the physically absorbed  $\text{NH}_3$ . Finally, the TPD experiment started with a heating rate of  $10^\circ\text{C}/\text{min}$ , and the  $\text{NH}_3$  desorption signal was detected by a thermal conductivity detector (TCD). Fourier transform infrared (FT-IR) spectra of catalysts were recorded on a NICOLET IS10 (Thermo SCIENTIFIC Company) in the spectral range of  $4000\text{--}450\text{ cm}^{-1}$  with a resolution of  $4\text{ cm}^{-1}$  using the conventional KBr pellet technique.

### 2.4 | Catalytic amination of benzene

To a 100 ml three-necked flask with reflux condenser, stirrer and a thermometer. The catalyst and  $\text{NH}_2\text{OH}\cdot\text{HCl}$  in proportion were loaded into the flask containing acetic acid aqueous solution, after stirring for 20 min at 30 °C,

22.5 mmol benzene was introduced, and the mixture was heated to the required temperature under agitation. After the reaction was carried out for 4 hrs, the resulting mixture was cooled to room temperature and neutralized by a 30% NaOH solution. The organic compounds were extracted with ether and analyzed by GC-MS (Agilent GC6890) equipped with a HP-5 capillary column (film thickness, 0.25  $\mu\text{m}$ ; i.d., 0.25 mm; length, 30 m) and flame ionization detector (FID) using n-butyl alcohol as an internal standard, and further identified by gas chromatography-mass spectrometry (Agilent, 5973 Network 6890 N) by comparing retention times and fragmentation patterns with authentic samples. The temperature of the GC column was set at 60  $^{\circ}\text{C}$  for 3 min and then was programmed to rise to 80  $^{\circ}\text{C}$  at the rate of 5  $^{\circ}\text{C}/\text{min}$ , and further reached 220  $^{\circ}\text{C}$  at the rate of 10  $^{\circ}\text{C}/\text{min}$  and remained at that temperature for 3 min.

### 3 | RESULTS AND DISCUSSION

#### 3.1 | Catalyst characterization

##### 3.1.1 | X-ray powder diffraction (XRD) studies

XRD diffraction peaks of the samples are shown in Figure 1. It can be seen that all the samples have typical AFI topology, the peaks of 100, 110, 200, 210, 002, 211, 220 were characterized of  $\text{AlPO}_4\text{-5}$ , and the crystallinity was high, and no diffraction peaks for other crystalline phases were found, which indicated that a single  $\text{NiAlPO}_4\text{-5}$  crystal was obtained in a given range of nickel

doping. According to Bragg formula, when the value of the crystal plane spacing ( $d$ ) is increased, it indicates that the small ion of the crystal structure is replaced by a large ion. For the same type of metal ions, the migration extent of  $d$  values reflects the amount of nickel substitution into the molecular sieve. The greater increasing of  $d$  is, the more of metal ions go into the molecular sieve framework, as shown in Figure 1, angle shifting to a small angle of Ni (0.3)  $\text{AlPO}_4\text{-5}$  sample (100) is the most obvious, it shows that the amount of Ni metal ions which isomorphously substitute  $\text{P}^{5+}$  in molecular sieve skeleton is the largest. This has been verified by the fact that, when the doping amount of Ni is 0.3, the catalyst shows the highest activity.

Figure 2 shows that the molecular sieve samples before and after calcination, the characteristic diffraction peaks (110), (200), (210) have the corresponding peak intensity. After calcination, the intensity of the (110) diffraction peak is enhanced, while the intensity of (100) and (210) is relatively weaker than that of the uncalcined due to the lattice distortion induced by the organic template. They all keep a typical topological structure of AFI.<sup>[36]</sup>

##### 3.1.2 | TG

The TG data of the as-synthesized  $\text{AlPO}_4\text{-5}$  and calcined  $\text{AlPO}_4\text{-5}$  in various nickel doping samples synthesized are presented in Figure 3 and Figure 4. The TG data of the calcined  $\text{AlPO}_4\text{-5}$  and  $\text{AlPO}_4\text{-5}$  samples presented in Figure 4 indicated that the largest amount of total weight loss during heating to 800  $^{\circ}\text{C}$  is 18.0%.

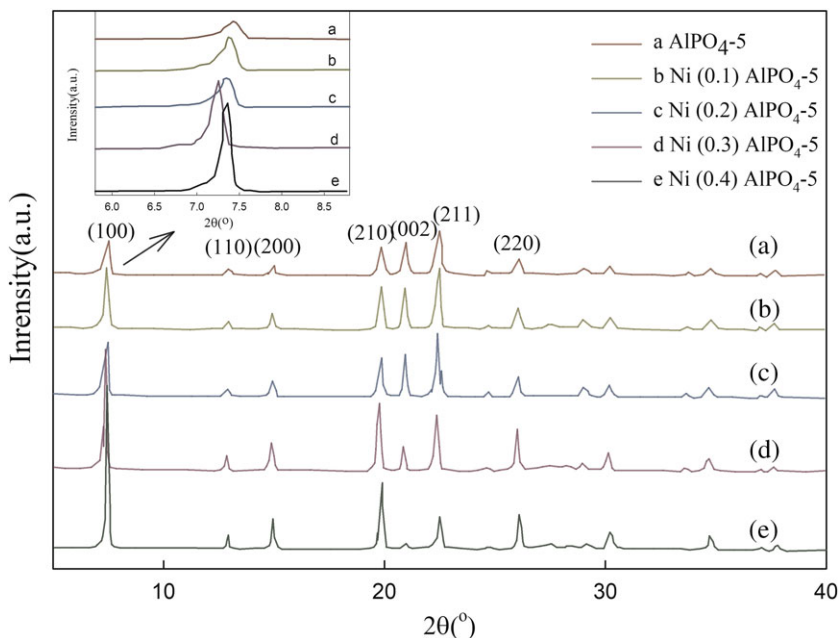


**FIGURE 1** XRD spectra of  $\text{NiAlPO}_4\text{-5}$  with various nickel doping

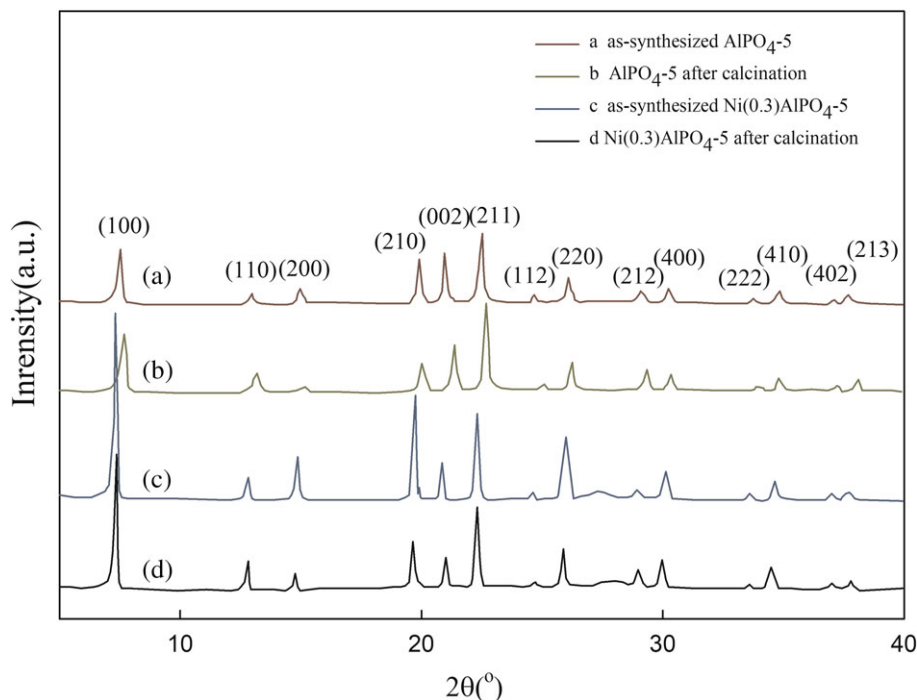


**FIGURE 2** XRD spectra of AlPO<sub>4</sub>-5 and NiAlPO<sub>4</sub>-5 before and after calcination

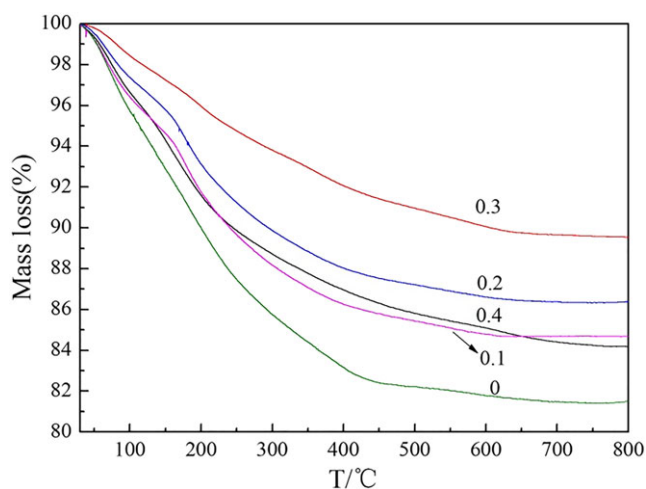


**FIGURE 3** TG spectra of as-synthesized AlPO<sub>4</sub>-5 in various nickel doping

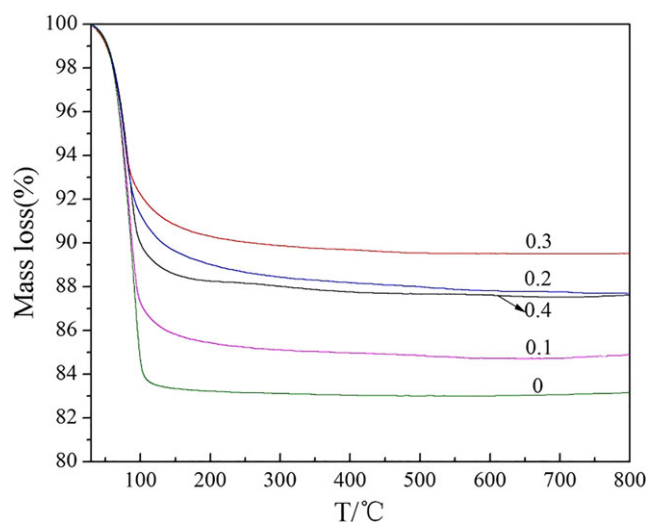


**FIGURE 4** TG spectra of calcined AlPO<sub>4</sub>-5 in various nickel doping

The weight loss of the as-synthesized AlPO<sub>4</sub>-5 and nickel substituted AlPO<sub>4</sub>-5 samples mainly includes the desorption of water molecules adsorbed in the molecular sieve and the depletion of the organic template agent. The first weight loss in the low temperature range 90 °C–100 °C with an endothermic process is assigned to the water desorption. Since the as-synthesized powders were dried at 90 °C for 16 hr, it is not obvious enough to observe this change from the figure. The second and third weight losses, both accompanied by an exothermic effect,

are attributed to the oxidative decomposition of organic template, suggesting that the template of TEA in the channel of AlPO<sub>4</sub>-5 and nickel containing AlPO<sub>4</sub>-5 samples may have different chemical environment. The template decomposition can be related to the dimensions of the channel system, the nature of the template, and the template–framework interaction.<sup>[37–39]</sup> By considering the strong template–framework interaction between protonated template and negatively charged framework, the second weight loss can be attributed to the removal of

neutral template molecule. While the third weight loss may be due to the decomposition of charged template molecule in the channel of as-synthesized molecular sieves.<sup>[37,40]</sup> It is concluded from the comparison that

the weight loss rate of Ni(0.3)AlPO<sub>4-5</sub> is the least, only about 10.0%. This shows that Ni(0.3)AlPO<sub>4-5</sub> molecular sieve has the best thermal stability among the AlPO<sub>4-5</sub> with various nickel doping.

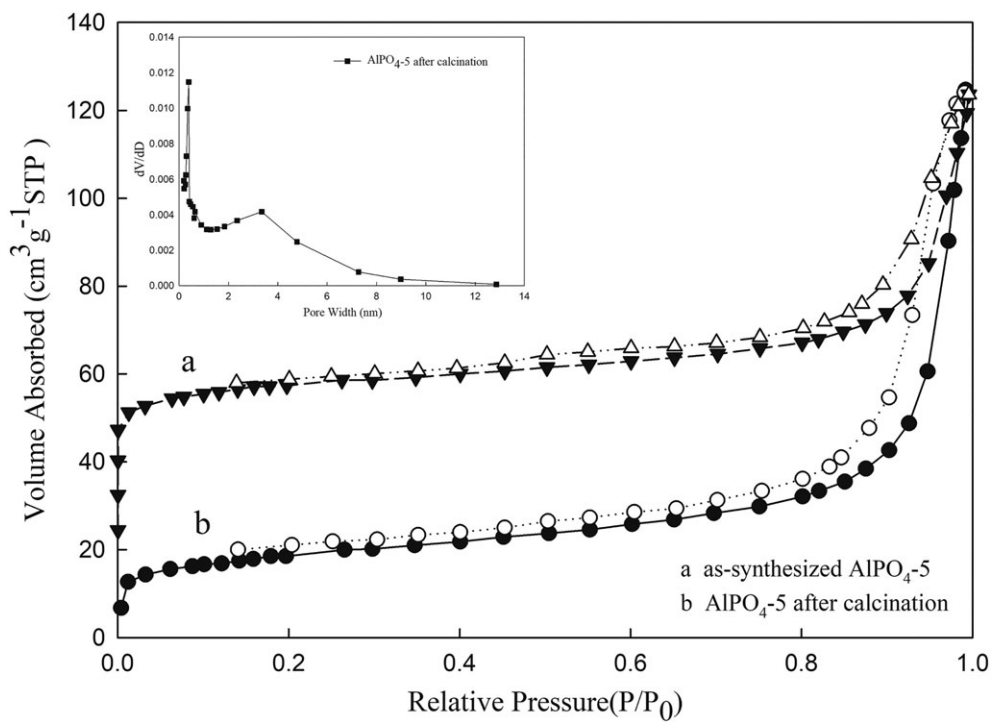


FIGURE 5 BET spectra of the as-synthesized and calcined AlPO<sub>4-5</sub>

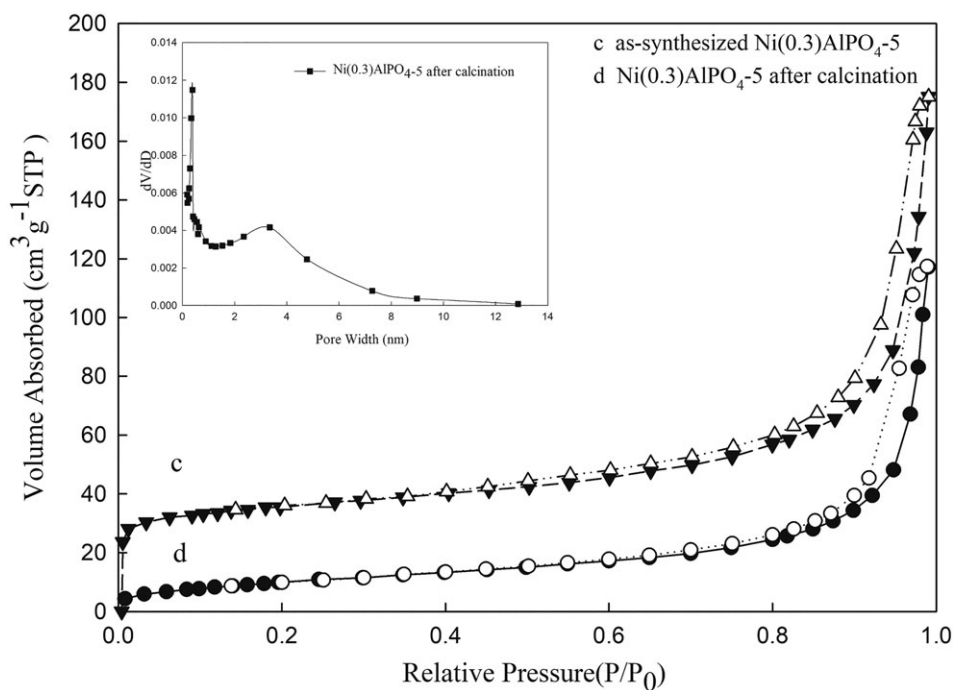


FIGURE 6 BET spectra of the as-synthesized and calcined Ni(0.3)AlPO<sub>4-5</sub>

### 3.1.3 | Bet

The adsorption and desorption isothermal curves for various catalysts were shown in Figure 5, 6 after calcination, the adsorption capacity increased rapidly in a relatively low pressure, characterizing of the single molecule layer adsorption. With the increasing of the relative pressure, the adsorption capacity increases slowly. As the pores were gradually filled by absorbed molecules, the adsorption capacity gradually decreased to show a platform-like area. This belongs to a typical monolayer or quasi monolayer adsorption characteristics. Capillary condensation phenomena occurred at  $P/P_0 = 0.2$  in the  $\text{AlPO}_4-5$  and  $P/P_0 = 0.7$  in the  $\text{Ni}(0.3)\text{AlPO}_4-5$ . The adsorption isothermal line and the desorption isothermal curve is no longer coincides with to result in the occurrence of hysteresis. For the samples, the narrowing of the hysteresis loop may be induced by the accumulation of particles in the framework of the molecular sieve for the partial nickel institution to change the structure of inner channel.

We also obtained the data of the molecular sieve surface area and the micro pore volume, the surface area of as-synthesized  $\text{AlPO}_4-5$  and  $\text{Ni}(0.3)\text{AlPO}_4-5$  were  $67.1 \text{ m}^2 \cdot \text{g}^{-1}$  and  $38.6 \text{ m}^2 \cdot \text{g}^{-1}$ , respectively, and the micropore volume was almost 0, with the pores to be occupied by water and organic template. After calcination, specific surface area of  $\text{AlPO}_4-5$  and  $\text{Ni}(0.3)\text{AlPO}_4-5$  was increased to  $194.7 \text{ m}^2 \cdot \text{g}^{-1}$  and  $123.4 \text{ m}^2 \cdot \text{g}^{-1}$ , and the micropore volume increased to  $0.07 \text{ cm}^3 \cdot \text{g}^{-1}$  and  $0.03 \text{ cm}^3 \cdot \text{g}^{-1}$ , respectively.

### 3.1.4 | SEM

The scanning electron microscopy (SEM) images of  $\text{AlPO}_4-5$  and  $\text{Ni}(0.3)\text{AlPO}_4-5$  are shown in Figure 7. Both the particles of  $\text{Ni}(0.3)\text{AlPO}_4-5$  and  $\text{AlPO}_4-5$  samples are presented in the form of small crystals aggregation. Despite they have slight difference in the degree of aggregation, the size and shape of the crystals are nearly of no difference. The particles of  $\text{Ni}(0.3)\text{AlPO}_4-5$  appear as clusters of hexagonal-shaped crystals with 5–10  $\mu\text{m}$  in size. And this morphology has been observed before in both the  $\text{AlPO}_4-5$ <sup>[21]</sup> and  $\text{CuAlPO}_4-5$ <sup>[41]</sup> systems.

### 3.1.5 | $\text{NH}_3$ -TPD

The acidity of the catalysts is evaluated via  $\text{NH}_3$ -TPD measurements. The results regrouped in Figure 8 shown a large peak located at 147 °C characterized to the

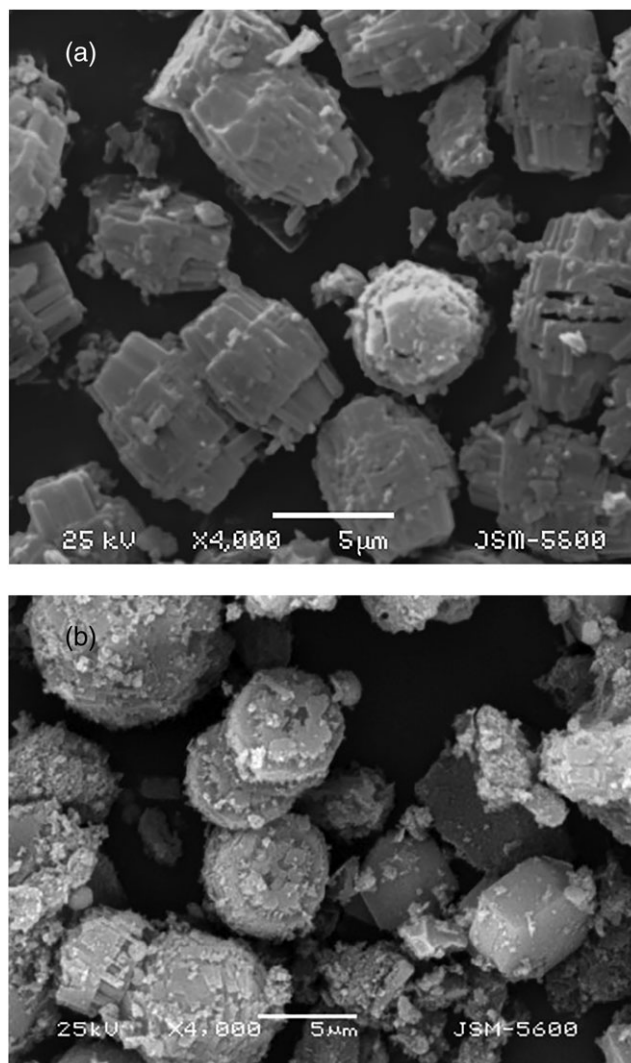


**FIGURE 7** (a) Scanning electron micrographs of  $\text{AlPO}_4-5$ . (b) Scanning electron micrographs of  $\text{Ni}(0.3)\text{AlPO}_4-5$

existence of weak acidic sites. It is seen that the peak intensity increased when the Ni is incorporated to the  $\text{AlPO}_4-5$  structure, this phenomenon is consistent with the results of our catalytic experiments, conversion of benzene, yield to aniline and selectivity to aniline increased in Ni content, among the catalysts,  $\text{Ni}(0.3)\text{AlPO}_4-5$  had the best effect. Continue to increase nickel content, the yield to byproduct biphenyl increased.

### 3.1.6 | Ft-IR

Figure 9 represents the FT-IR spectra of the catalysts. The vibration band at  $3500\text{--}3400 \text{ cm}^{-1}$  observed in all samples is assigned to H–O–H bending motion of adsorbed water. As can be discerned, the spectra of all samples exhibit

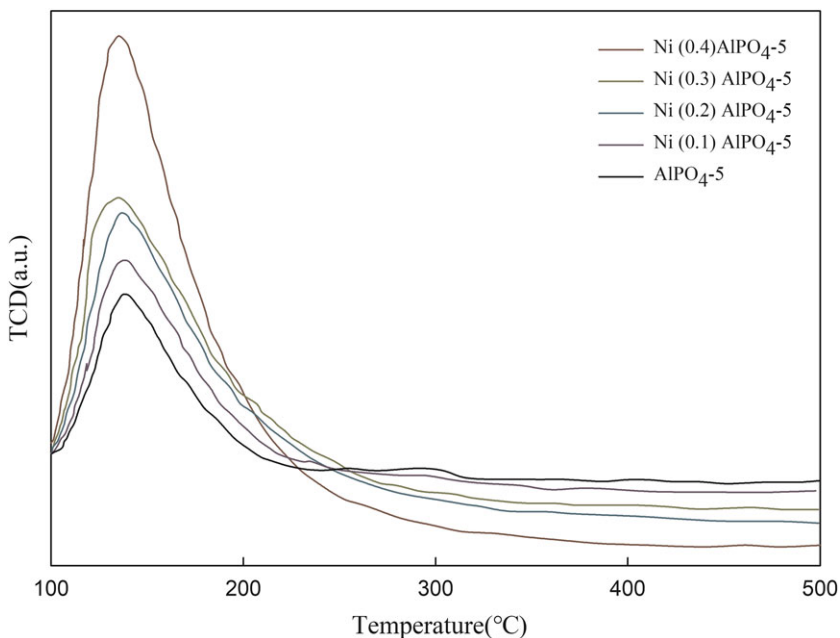


**FIGURE 8** NH<sub>3</sub>-TPD of AlPO<sub>4</sub>-5 in various nickel doping

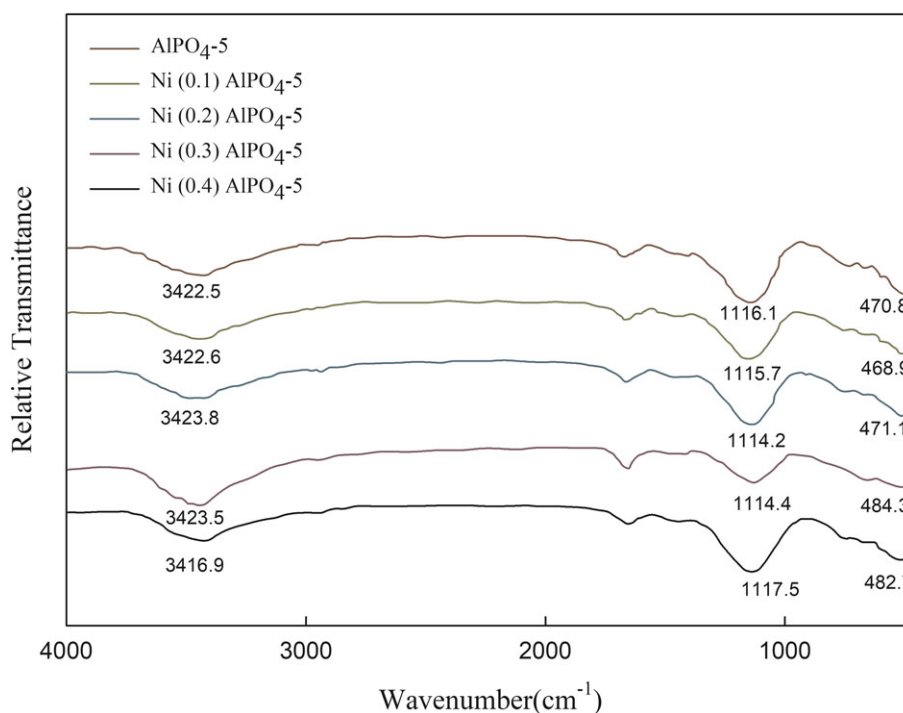


**FIGURE 9** FTIR of AlPO<sub>4</sub>-5 in various nickel doping

broad absorption bands in the range of 1100–1130  $\text{cm}^{-1}$ , which correspond to the asymmetric vibration of phosphate (triple degenerate P-O stretching vibration).<sup>[42]</sup> Besides, the bands at 470–490  $\text{cm}^{-1}$ , 640–650  $\text{cm}^{-1}$ , 860–875  $\text{cm}^{-1}$  for the catalysts are the Al-O-P stretching vibrations as well as the O-P-O bending mode of the  $\text{PO}_4^{3-}$  tetrahedral, respectively,<sup>[43]</sup> indicating the presence of crystalline AlPO<sub>4</sub> that is also corroborated by the XRD analysis.

## 3.2 | Amination activity evaluation of the catalyst

### 3.2.1 | The influence of nickel doping amount

Various nickel-doped AlPO<sub>4</sub>-5 catalysts were tested for the direct amination of benzene, the results are summarized in Table 1.

**TABLE 1** Catalyst performance over NiAlPO<sub>4-5</sub> catalysts

Catalyst	n (NH <sub>2</sub> OH·HCl)/ n(C <sub>6</sub> H <sub>6</sub> )	Acetic acid (vol.%)	C <sub>6</sub> H <sub>6</sub> Conv. (%) <sup>a</sup>	Yield		Aniline Selec <sup>d</sup> (%)
				Aniline <sup>b</sup> (%)	Byproduct <sup>c</sup> (%)	
IPO <sub>4-5</sub>	1/1	70.0	4.7	3.5	0.8	78.4
Ni(0.1)AlPO <sub>4-5</sub>	1/1	70.0	39.5	33.4	0.4	90.1
Ni(0.2)AlPO <sub>4-5</sub>	1/1	70.0	52.8	49.7	0.4	94.2
Ni(0.3)AlPO <sub>4-5</sub>	1/1	70.0	73.2	73.2	0.0	100.0
Ni(0.4)AlPO <sub>4-5</sub>	1/1	70.0	75.5	69.6	1.1	92.2
Ni(0.3)AlPO <sub>4-5</sub>	1/1	50.0	50.5	43.2	0.2	85.4
Ni(0.3)AlPO <sub>4-5</sub>	1/1	60.0	58.8	54.2	0.3	92.2
Ni(0.3)AlPO <sub>4-5</sub>	1/1	80.0	80.2	59.1	8.2	73.8
Ni(0.3)AlPO <sub>4-5</sub>	0.5/1	70.0	59.9	57.2	0.1	95.8
Ni(0.3)AlPO <sub>4-5</sub>	1/1.5	70.0	75.6	65.1	0.2	86.5
Ni(0.3)AlPO <sub>4-5</sub>	2/1	70.0	82.4	58.0	5.5	70.4

Reaction condition: Benzene: 22.5 mmol (2.0 ml), time: 4 hr, temperature: 80 °C, catalyst input: 0.1 g.

<sup>a</sup>Conversion of benzene (%) = [converted benzene amount (mol) /initial amount (mol) of benzene] × 100%;

<sup>b</sup>Yield of aniline (%) = [amount (mol) of aniline/ initial amount (mol) of benzene] × 100%;

<sup>c</sup>Yield of byproduct (%) = [amount (mol) of byproduct/initial amount (mol) of benzene] × 100% and the by-product was detected as biphenyl;

<sup>d</sup>Selectivity to aniline (%) = {converted amount (mol) of benzene to aniline/initial amount of benzene} × 100%.

When AlPO<sub>4-5</sub> was used as a catalyst, the conversion of benzene is 4.7%, and the selectivity to aniline was 78.4%. The conversion of benzene and the selectivity to aniline with nickel doped catalysts were significantly higher than those of AlPO<sub>4-5</sub> catalyst, this is due to introduction of nickel ions in the framework of AlPO<sub>4-5</sub>. When the nickel doping increased from 0.1 to 0.3, the conversion of benzene increased from 39.5% to 73.2%, with further increasing in nickel doping, the conversion increases to 75.5%, but the selectivity decreases to 92.2%. Combined with XRD, BET and FI-IR analysis, it can be concluded that excess nickel

doping will make the particles accumulate in the catalyst to block its pores, hindering the diffusion and reaction. Therefore, the catalysts used in the following experiments were Ni(0.3)AlPO<sub>4-5</sub>.

### 3.2.2 | The influence of reaction temperature

The effect of the reaction temperature on amination of benzene was shown in Figure 10.

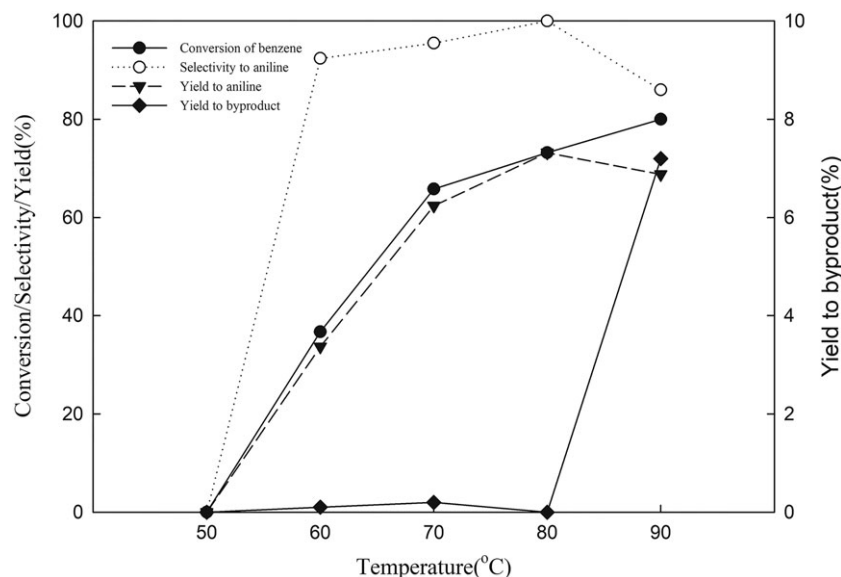
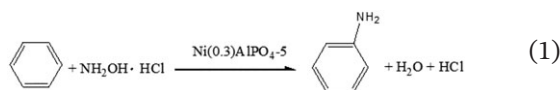


**FIGURE 10** Effect of reaction temperature on the amination

When the temperature was 50 °C, there was no aniline, it indicated that the catalyst was not active. When the reaction temperature rose from 60 to 80 °C, the yield of aniline increased from 33.7% to 67.2%, further temperature increasing makes the yield decrease to 43.8%. Higher temperature could accelerate the decomposition of hydroxylamine and benzene volatilization,<sup>[2]</sup> it is also possible that aniline was further oxidized to form by-products, witnessed by the nitrobenzene's presence in the product. It can be determined that the appropriate reaction temperature is 80 °C.

### 3.2.3 | Kinetics of aniline synthesis by amination of benzene

In aniline synthesis from benzene with hydroxylamine hydrochloride, Ni(0.3)AlPO<sub>4</sub>-5 as catalyst, the reaction process could be described by following expression:



The reaction rate equation could describe as:

$$r = -\frac{dc_A}{dt} = kc_A^\alpha c_B^\beta = k[c_{A0}(1-x)]^\alpha \left[ c_{A0} \left( 1 - \frac{1}{2}x \right) \right]^\beta \quad (2)$$

Where  $r$  is the reaction rate in terms of the rate of consumption of benzene,  $c_{A0}$  is the initial concentration of benzene,  $c_A$  and  $c_B$  represent the instantaneous molar concentrations of benzene and hydroxylamine hydrochloride, respectively. The  $\alpha$  and  $\beta$  are the reaction order of the corresponding concentration factor,  $t$  is the reaction time,  $k$  is the reaction rate constant,  $x$  is the measured conversion of benzene.

The reaction kinetics of aniline synthesis was investigated at three temperatures of 313.15 K, 323.15 K and 333.15 K. The conversion  $x$  of the reaction system at each time is substituted into the integral formula, and the time  $t$  is plotted as Figure 11.

The linear relationship in the figure is obvious, that is, the direct catalyzed synthesis of aniline by benzene shows a grade 1 for benzene. The slope of each line in the figure is the apparent rate constant  $k$  at that temperature. The Arrhenius equation to  $k$  rate constant into  $\ln k$  and Plot  $1/T$  and the result is shown in Figure 12. From the obtained parameters, the kinetic equations are sorted out:

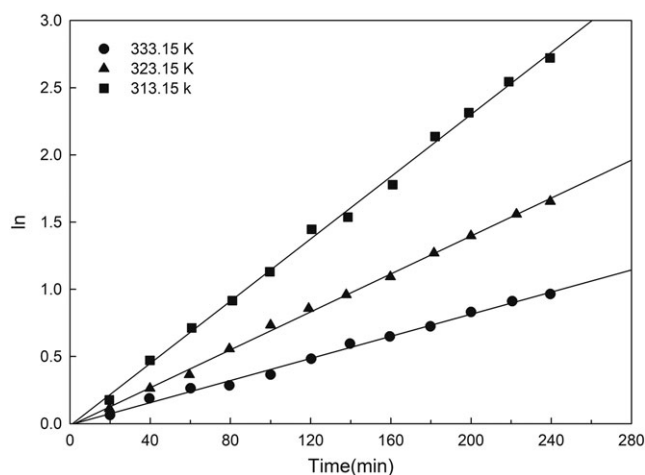


FIGURE 11 Relation between integrals  $\ln$  and time at various temperatures

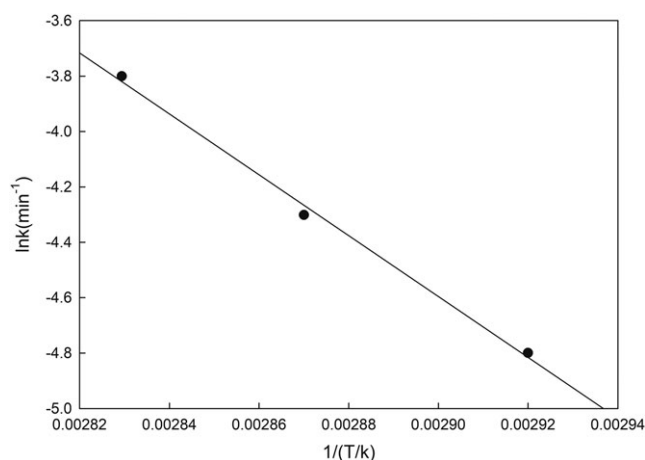


FIGURE 12 Effect of temperature on apparent reaction rate constant

$$r = -\frac{dc_A}{dt} = 2.258 \times 10^{13} e^{-\frac{101389}{RT}} c_A \quad (\text{min}^{-1})$$

### 3.2.4 | The influence of the acidity of the reaction medium

The effect of the acidity of the reaction medium on amination of benzene is shown in Table 1.

The  $\text{pK}_a$  of the  $\bullet\text{NH}_3^+$  is 3.75 and 6.7,<sup>[42]</sup> which indicates that in a relative acidic reaction system,  $\bullet\text{NH}_3^+$  is the dominant position comparing to neutral amino acid group. Kuznetsova<sup>[16]</sup> put forward a free-radical mechanism, considering the protonation of amino radical ( $\bullet\text{NH}_3^+$ ) as the activity group for amination by an initio quantum mechanics calculations for the amination of benzene and toluene. In acetic acid solution, hydroxylamine exists in the form of  $\text{HONH}_3^+$ , acting as a reducing

agent,<sup>[43]</sup> the reduction of hydroxylamine by the catalyst will generate  $\bullet\text{NH}_3^+$  and then, it reacts with benzene to form protonated aminocyclohexadienyl intermediates. Due to its instability, it is easily oxidized into aniline. This shows that a relative acidic condition is favorable to the amination of benzene. No aniline was generated when only water or only acetic acid was used as the solvent. When acetic acid aqueous solution is employed, as hydroxylamine can easily dissolve in it, the increasing of concentration of acetic acid make selectivity to aniline increase, when the concentration is vol. 70.0%, aniline selectivity reached 100%, continuing to increase the concentration of acetic acid, the conversion of benzene and selectivity to aniline both decreased. This shows that vol. 70.0% acetic acid solution is an appropriate reaction medium.

### 3.2.5 | The influence of the ratio of raw materials

The effect of the ratio of raw materials on the amination is shown in Table 1.

When the molar ratio of the reactants  $n_{\text{NH}_2\text{OH}\cdot\text{HCL}}/n_{\text{benzene}}$  increased from 0.5: 1 to 1: 1, selectivity to aniline rose from 95.8% to 100%, benzene conversion increased from 59.9% to 73.2%, and when the reactant ratio increased from 1: 1 to 2: 1, benzene conversion increased slowly from 73.2% to 75.6%, while selectivity to aniline significantly reduced from 100% to 86.5%, which may be the reason that excess amount of hydroxylamine in the solution led to accelerate its decomposition to produce  $\text{N}_2\text{O}$  by nickel catalyst<sup>[2]</sup> and the yield to byproduct biphenyl increased. When the reactant ratio  $n_{\text{NH}_2\text{OH}\cdot\text{HCL}}/n_{\text{benzene}}$  is 1:1, the

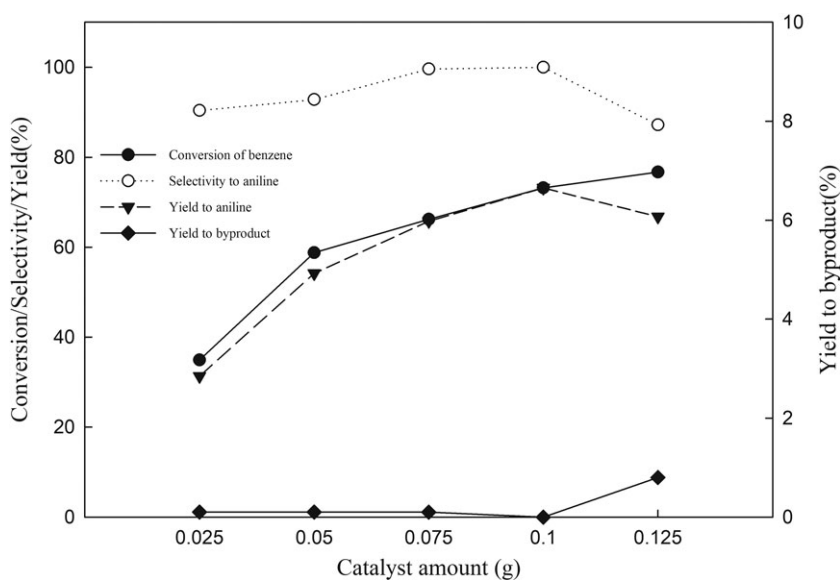


FIGURE 13 Effect of catalyst input on amination of benzene

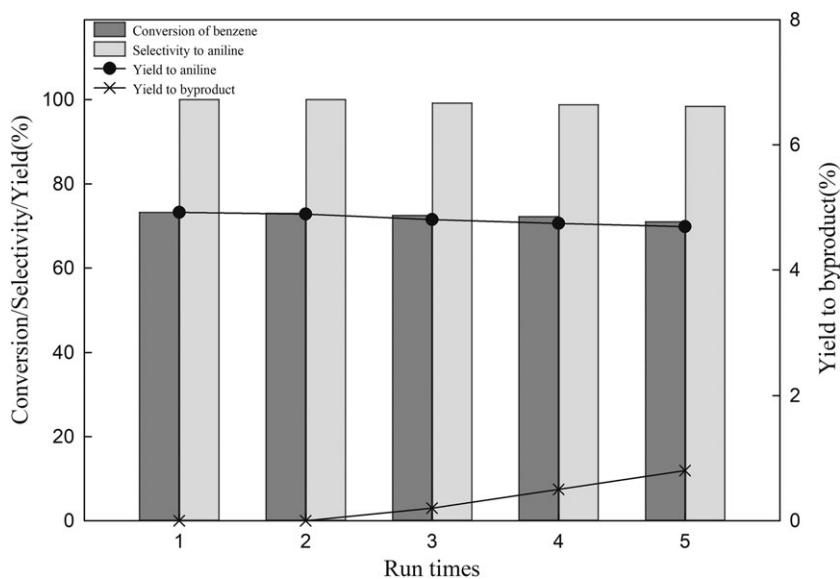


FIGURE 14 Recyclability of the catalyst on amination

selectivity to aniline reaches the maximum, so it is chosen as a suitable ratio of raw materials.

### 3.2.6 | The influence of catalyst input

The influence of catalyst input on the amination is shown in Figure 13.

When no catalyst was added, no aniline was generated, as the catalyst input was increased from 0.025 g to 0.1 g, the benzene conversion increased from 34.9% to 73.2%, and the selectivity to aniline increased from 89.4% to 100%. Continuing to increase the catalyst input, the conversion of benzene increased from 73.2% to 76.7%, while the selectivity to aniline decreased from 100% to 87.1%. The analysis of the reaction products shows that by-products of nitrobenzene and the minor others have generated. Therefore, the optimal input of catalyst is 0.1 g.

### 3.2.7 | Optimal process conditions and recyclability of the catalyst

According to the above results, the optimum reaction conditions were as follows:  $n_{\text{NH}_2\text{OH}\cdot\text{HCL}}/n_{\text{benzene}}$  was 1:1, Ni (0.3)  $\text{AlPO}_4\text{-5}$  was 0.1 g, in vol. 70.0% acidic medium at 80 °C and atmospheric pressure, and the selectivity to aniline was 100.0% and the yield was 73.2%. Under these conditions, the Ni(0.3) $\text{AlPO}_4\text{-5}$  was used for recycling study, after the first run, the catalyst was separated by filtration, washed 3 times with distilled water, dried at 100 °C and reused in the reaction with a fresh reaction mixture. After five runs, the activity change is shown in Figure 14.

It is seen that the yield of aniline decreased by 2.0%, and the selectivity to aniline was 1.5% after five runs. This indicated that the catalytic performance of the catalyst was stable and has potential for further development.

## 4 | CONCLUSION

A series of Ni $\text{AlPO}_4\text{-5}$  was prepared by hydrothermal method with the same crystal structure and high crystallinity of  $\text{AlPO}_4\text{-5}$  and were used in the direct amination of benzene to prepare aniline for the first time. Structural analyses show that phosphorus ions were isomorphously substituted by nickel metallic ions. Nickel doping amount has prominent effect on the properties and activity of the catalyst, with 0.3 doping amount to be the best. The optimized amination conditions were as follow: $n_{\text{NH}_2\text{OH}\cdot\text{HCL}}/n_{\text{benzene}}$  1:1, vol. 70.0% acetic acid solution, temperature 80 °C, time 4 hr, under atmospheric pressure, Ni(0.3)

$\text{AlPO}_4\text{-5}$  as the catalyst, with aniline yield of 73.2% and 100% selectivity to aniline. And this catalyst can be used up to five cycles with little activity declining. This process has great potential in industry exploration.

## ACKNOWLEDGEMENTS

The authors gratefully acknowledge Changchun University of Technology for all of the support that was provided.

## ORCID

Long Zhang  <https://orcid.org/0000-0002-5719-135X>

## REFERENCES

- [1] L. Schmerling, U. S. Patent. No. 2948755, **1960**.
- [2] L. F. Zhu, B. Guo, D. Y. Tang, X. K. Hu, G. Y. Li, C. W. Hu, *J. Catal.* **2007**, 245, 446.
- [3] B. R. Thomas, T. William, *Science* **1999**, 284, 1477.
- [4] J. Becker, J. P. M. Niederer, M. Keller, W. F. Hölderich, *Appl. Catal. A. Gen.* **2000**, 197, 229.
- [5] R. S. Downing, P. J. Kunkeler, H. VanBekum, *Catal. Today* **1997**, 37, 121.
- [6] T. Chen, C. W. Hu, Z. J. Fu, A. Tian, *Chin. Sci. Bull.* **2002**, 47, 1937.
- [7] P. T. Anastas, L. B. Bartlett, M. M. Kirchhoff, T. C. Williamson, *Catal. Today* **2000**, 55, 11.
- [8] W. D. Jones, *Science* **2000**, 287, 1942.
- [9] C. Jia, D. Piao, J. Oyamada, W. Lu, T. Kitamura, Y. Fujiwara, *Science* **2000**, 287, 1992.
- [10] H. Chen, S. Schlecht, T. C. Semple, J. F. Hartwig, *Science* **2000**, 287, 1995.
- [11] S. I. Niwa, M. Eswaramoorthy, J. Nair, A. Raj, N. Itoh, H. Shoji, T. Namba, F. Mizukami, *Science* **2002**, 295, 105.
- [12] A. Hagemeyer, R. Borade, P. Desrosiers, S. H. Guan, D. M. Lowe, D. M. Poojary, H. Turner, H. Weinberg, X. P. Zhou, R. Armbrust, G. Fengler, U. Notheis, *Appl. Catal. A. Gen.* **2002**, 227, 43.
- [13] P. Desrosiers, S. H. Guan, A. Hagemeyer, D. M. Lowe, C. Lugmair, D. M. Poojary, H. Turner, H. Weinberg, X. P. Zhou, R. Armbrust, G. Fengler, U. Notheis, *Catal. Today* **2003**, 81, 319.
- [14] D. M. Poojary, R. Borade, A. Hagemeyer, X. P. Zhou, C. E. Dube, U. Notheis, R. Armbrust, C. Rasp, D. M. Lowe, U. S. Patent. No. 6933409, **2005**.
- [15] M. A. Mantegazza, G. Leofanti, G. Petrini, M. Padovan, A. Zecina, S. Bordiga, *Stud. Surf. Sci. Catal.* **1994**, 82, 541.
- [16] N. I. Kuznetsova, L. I. Kuznetsova, L. G. Detusheva, V. A. Likhobolov, G. P. Pez, H. Cheng, *J. Mol. Catal. A.* **2000**, 161, 1.
- [17] Y. F. Lü, L. F. Zhu, Q. Y. Liu, B. Guo, X. K. Hu, C. W. Hu, *Chin. Chem. Lett.* **2009**, 20, 238.

- [18] K. M. Parida, Saswati Soumya Dash, S. Singha, *Appl. Catal. A-Gen.* **2008**, *351*, 59.
- [19] R. Xu, W. Pang, J. Yu, Q. Huo, J. Chen, *Chemistry of zeolites and related porous materials: synthesis and structure*, John Wiley & Sons, Ltd, Chichester, UK **2007**.
- [20] G. Basina, D. AlShami, K. Polychronopoulou, V. Tzitzios, V. Balasubramanian, F. Dawaymeh, G. N. Karanikolos, Y. A. Wahedi, *Surf. Coat. Technol.* **2018**, *353*, 378.
- [21] S. T. Wilson, B. M. Lok, C. A. Messina, T. R. Cannan, E. M. Flanigen, *J. Am. Chem. Soc.* **1982**, *104*, 1146.
- [22] M. Hartmann, L. Kevan, *Chem. Rev.* **1999**, *99*, 635.
- [23] H. Nur, H. Hamdan, *Mater. Res. Bull.* **2001**, *36*, 315.
- [24] G. Lischke, B. Parlitz, U. Lohse, E. Schreier, R. Fricke, *Appl. Catal. A-Gen.* **1908**, *166*, 351.
- [25] P. E. Dai, R. H. Petty, C. W. Ingram, R. Szostak, *Appl. Catal. A-Gen.* **1996**, *143*, 101.
- [26] S. T. Wilson, S. Oak, U.S. Patent No. 4567029, **1986**.
- [27] H. Hentita, A. Boudjemaa, A. Bouchama, J. C. Jumas, K. Bachari, M. S. Ouali, *Mater. Res. Bull.* **2018**, *106*, 418.
- [28] G. Finger, J. Kornatowski, K. Jancke, R. Matschat, W. H. Baur, *Micropor. Mesopor. Mat.* **1999**, *33*, 127.
- [29] V. R. Choudhary, D. B. Akocekar, S. D. Sansare, *Mater. Chem. Phys.* **1987**, *18*, 245.
- [30] H. X. Zhang, A. Chokkalingam, P. V. Subramaniam, S. Joseph, S. Takeuchi, M. D. Wei, A. M. Al-Enizi, H. G. Jang, J. H. Kim, G. Seo, K. Komura, Y. Sugi, A. Vinu, *J. Mol. Catal. A-Chem.* **2016**, *412*, 117.
- [31] F. Y. Jiang, J. P. Zhai, J. T. Ye, J. R. Han, Z. K. Tang, *J. Cryst. Growth* **2005**, *283*, 108.
- [32] A. M. Prakash, M. Hartmann, Z. D. Zhu, L. Kevan, *J. Phys. Chem. B* **2000**, *104*, 1610.
- [33] W. B. Fan, B. B. Fan, M. G. Song, T. H. Chen, R. F. Li, T. Dou, T. Tatsumi, B. M. Weckhuysen, *Micropor. Mesopor. Mat.* **2006**, *94*, 348.
- [34] R. W. Thompson, K. C. Franklin, H. Robson, K. P. Lillerud, *J. Crystallogr.* **2001**, *56*, 90.
- [35] A. Iwasaki, T. Sano, T. Kodaira, Y. Kiyozumi, *Micropor. Mesopor. Mat.* **2003**, *64*, 145.
- [36] C. Montes, M. E. Davis, B. Murray, M. Narayana, *J. Phys. Chem.* **1990**, *94*, 6425.
- [37] Y. Wei, Y. He, D. Zhang, L. Xu, S. Meng, Z. Liu, B. L. Su, *Microporous Mesoporous Mater.* **2006**, *90*, 188.
- [38] L. Zhang, J. N. Primera-Pedrozo, A. J. Hern'andezMaldonado, *J. Phys. Chem. C* **2010**, *114*, 14755.
- [39] Y. Wei, D. Zhang, L. Xu, F. Chang, Y. He, S. Meng, B. Su, Z. Liu, *Catal. Today* **2008**, *131*, 262.
- [40] F. M. Shalmani, R. Halladj, S. Askari, *RSC Adv.* **2017**, *7*, 26756.
- [41] T. Muñoz, A. M. Prakash, L. Kevan, K. J. Balkus, *J. Phys. Chem. B* **1998**, *102*, 1379.
- [42] A. Citterio, A. Gentile, F. Minisci, V. Navarrini, M. Serravalle, S. Ventura, *J. Org. Chem.* **1984**, *49*, 4479.
- [43] C. Wei, S. R. Saraf, W. J. Rogers, M. S. Mannan, *Thermochim. Acta* **2004**, *421*, 1.

**How to cite this article:** Wang W, Yang Y, Zhang L. Research on the direct amination of benzene to aniline by NiAlPO<sub>4</sub>-5 catalyst. *Appl Organometal Chem.* 2019;e4828. <https://doi.org/10.1002/aoc.4828>